Coupled Systems Mechanics, *Vol. 7, No. 1 (2018) 27-42*
DOI: https://doi.org/10.12989/csm.2018.7.1.027

Failure mechanisms in coupled soil-foundation systems

Emina Hadzalic[1,2a], Adnan Ibrahimbegovic[*1] and Samir Dolarevic[2b]

[1]*Université de Technologie de Compiègne/Sorbonne Universités, Laboratoire Roberval de Mecanique, Centre de Recherche Royallieu, 60200 Compiègne, France*
[2]*Faculty of Civil Engineering, University of Sarajevo, Patriotske lige 30, Sarajevo 71000, Bosnia and Herzegovina*

(Received February 25, 2017, Revised March 14, 2017, Accepted March 21, 2017)

Abstract. Behavior of soil is usually described with continuum type of failure models such as Mohr-Coulomb or Drucker-Prager model. The main advantage of these models is in a relatively simple and efficient way of predicting the main tendencies and overall behavior of soil in failure analysis of interest for engineering practice. However, the main shortcoming of these models is that they are not able to capture post-peak behavior of soil nor the corresponding failure modes under extreme loading. In this paper we will significantly improve on this state-of-the-art. In particular, we propose the use of a discrete beam lattice model to provide a sharp prediction of inelastic response and failure mechanisms in coupled soil-foundation systems. In the discrete beam lattice model used in this paper, soil is meshed with one-dimensional Timoshenko beam finite elements with embedded strong discontinuities in axial and transverse direction capable of representing crack propagation in mode I and mode II. Mode I relates to crack opening, and mode II relates to crack sliding. To take into account material heterogeneities, we determine fracture limits for each Timoshenko beam with Gaussian random distribution. We compare the results obtained using the discrete beam lattice model against those obtained using the modified three-surface elasto-plastic cap model.

Keywords: discrete beam lattice model; modified three-surface elasto-plastic cap model; Timoshenko beam; Gaussian distribution; failure mechanisms

1. Introduction

Nonlinear behavior of soil subjected to extreme loading is highly complex, with numerous factors affecting the final response. To take into account inelastic behavior and all the phenomena that can occur in different types of soils exposed to extreme loading, the phenomenological constitutive model requires a large number of parameters. For a more successful application in engineering practice, the model should be described with only few parameters that have clear physical meaning and that can be obtained from standard tests. In addition, numerical

∗Corresponding author, Chair for Computational Mechanics, Professor,
E-mail: adnan.ibrahimbegovic@utc.fr
[a]Ph.D., E-mail: emina.hadzalic@utc.fr or emina.hadzalic@gf.unsa.ba
[b]Professor, E-mail: samir.dolarevic@gf.unsa.ba

http://www.techno-press.org/?journal=csm&subpage=8 ISSN: 2234-2184 (Print), 2234-2192 (Online)

order to better take into account material heterogeneities, we determine fracture limits for each Timoshenko beam with Gaussian random distribution. We compare the results obtained with the discrete beam lattice model against those provided by a modified three-surface elasto-plastic cap model (Dolarevic and Ibrahimbegovic 2007).

The outline of the paper is as follows: In Section 2, we describe the discrete beam lattice model and give a short overview of finite element formulation for a Timoshenko beam finite element with embedded discontinuity in axial and transverse direction. In section 3, we give a short overview of modified three-surface elasto-plastic cap model. In section 4, we give a set of numerical examples where we compare the macroscale responses obtained with the discrete beam lattice model and modified three-surface elasto-plastic cap model. In section 5, we give concluding remarks.

2. Discrete beam lattice model

In the discrete beam lattice model proposed in (Nikolic *et al*. 2015) a solid body is represented as an assembly of one-dimensional Timoshenko beam finite elements with embedded strong discontinuity in axial and transverse direction capable of representing crack propagation in mode I and mode II. The meshing of the domain is done using Delaunay triangulation (Edelsbrunner 2001). Delaunay triangulation is based on the Delaunay criterion. This criterion, also called the empty circum-circle criterion, states that the cirum-circle associated with each triangle does not contain vertices of any other triangle in its interior. The end result of Delaunay triangulation is a mesh of triangles. The discrete model of a solid body is obtained by positioning Timoshenko beam finite elements along the edge of every Delaunay triangle. Cross sectional properties of the Timoshenko beams are determined from Voronoi diagram. For a given set of points, Voronoi diagram divides the region into a set of subregions or Voronoi cells. Voronoi cell is a set of all points that are the closest to the given point than to any other point. One of the most important property of the Voronoi discretization is that it can represent homogenized linear elastic responses. Here, we extend this goal further to representing the corresponding failure mechanisms. Namely, we first recall that Delaunay triangulation is dual to Voronoi cell representation. In other word, a center of every Voronoi cell is at the same time a vertex of a Delaunay triangle. For this reason, Voronoi diagram is constructed from a set of points that corresponds to the vertices of triangles obtained from the Delaunay triangulation. Each Timoshenko beam connects centers of two neighboring Voronoi cells and is perpendicular to their shared edge. The height of the cross section of any Timoshenko beam can then be determined from the length of that shared edge. This kind of cross section properties computation has been successfully used previously in (Ibrahimbegovic and Delaplace 2003). The discrete lattice model constructed in this way can successfully reproduce the linear elastic response of the equivalent standard continuum model as shown in (Nikolic *et al*. 2015). What needs to be emphasized is that the center of the Timoshenko beam is located at the edge shared between two neighboring Voronoi cells. This is a very convenient property for simulating crack propagation in materials. If we see Voronoi cells as parts of the material that are held together with cohesive links, then cracks in mode I and/or mode II can only occur at their interconnection. Next, we give governing equations for inelastic Timoshenko beam with enhanced kinematics. More details can be found in (Ibrahimbegovic 2009, Nikolic *et al*. 2015, Nikolic and Ibrahimbegovic 2015, Do *et al*. 2015, Imamovic *et al*. 2015).

2.3 Constitutive equations

The constitutive law for a Timoshenko beam finite element in axial and transverse direction consists of three parts (Fig. 1). The first part is the linear elastic part described with Hooke's linear elastic law. After reaching the yield limit, the behavior of the element is governed by plasticity with linear isotropic hardening. Post-peak behavior of an element is described with exponential softening. Behavior of the element in bending in all three parts is linear elastic.

Governing equations for plasticity with linear isotropic hardening:

-Additive decomposition of total deformation in elastic ε^e and plastic part ε^p:

$$\varepsilon = \varepsilon^e + \varepsilon^p$$

-Strain energy function in terms of strains ε and internal variables, plastic deformation ε^p and strain-like hardening variable ξ:

$$\psi\left(\varepsilon, \varepsilon^p, \xi\right) = \frac{1}{2}\left(\varepsilon - \varepsilon^p\right) C \left(\varepsilon - \varepsilon^p\right) + \frac{1}{2} \xi K \xi$$

where C is the elastic constant (E or G), and K the hardening modulus.

-Yield function in terms of stress σ and dual variable q:

$$\phi(\sigma, q) = |\sigma| - \left(\sigma_y - q\right) \leq 0$$

where σ_y is the yield limit, and $q = K\xi$ is a stress-like variable.

-Evolution equations for internal variables ε^p and ξ:

$$\frac{\partial \varepsilon^p}{\partial t} = \frac{\partial \overline{\gamma}}{\partial t} sign(\sigma), \ \frac{\partial \xi}{\partial t} = \frac{\partial \overline{\gamma}}{\partial t}$$

where $\overline{\gamma}$ is the plastic multiplier.

-Loading/unloading conditions:

$$\frac{\partial \overline{\gamma}}{\partial t} \geq 0, \ \phi \leq 0, \ \frac{\partial \overline{\gamma}}{\partial t} \phi = 0$$

-Consistency condition:

$$\frac{\partial \overline{\gamma}}{\partial t} \frac{\partial \phi}{\partial t} = 0$$

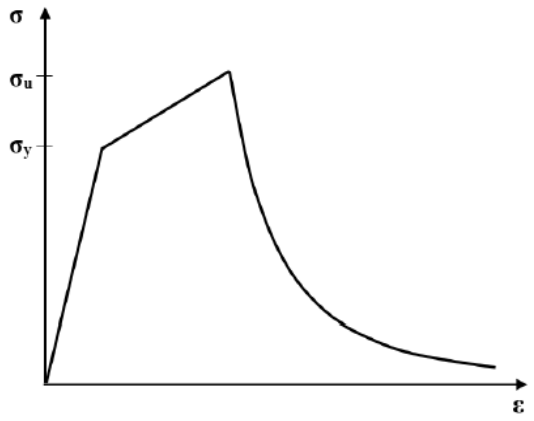

Fig. 1 Constitutive model for Timoshenko beam finite element for axial and transverse direction

specimen, while the second invariant of the deviatoric part J_2 controls the change in the shape of the specimen.

$$I_1 = tr[\boldsymbol{\sigma}] \tag{10}$$

$$\sqrt{J_2} = \|\mathrm{dev}[\boldsymbol{\sigma}]\| \tag{11}$$

The Drucker-Prager loading function for the modified cap model is written as

$$f_1(I_1, J_2) = \alpha I_1 + \sqrt{J_2} - k = 0,\ I_1^T \le I_1 \le I_1^c \tag{12}$$

where α and k are strength parameters specifying soil cohesion and angle of internal friction.

The strain-hardening elliptic cap function is written as

$$f_2\left(I_1, J_2, \xi\left(\varepsilon_v^p\right)\right) = \frac{(I_1 - a)^2}{R^2 f_{dp}(a)} + J_2 - \mathrm{b}^2 = 0,\ I_1 \ge I_1^c \tag{13}$$

where $\xi\left(\varepsilon_v^p\right)$ is the hardening law defined with

$$\xi\left(\varepsilon_v^p\right) = \frac{1}{D} ln\left(1 + \frac{\varepsilon_v^p}{W}\right) \tag{14}$$

In previous equations, R, W and D are hardening material parameters, $a(\xi)$ is an ordinate of the ellipse center, $b(\xi)$ is the main radius of the ellipse.

The function for the third surface i.e., the cut-off plane is written as

$$f_3(I_1, J_2) = (I_1 - T + R_T)^2 = R_T^2,\ I_1 \le I_1^T \tag{15}$$

where T is the tension cut-off limit, and R_T is the radius center.

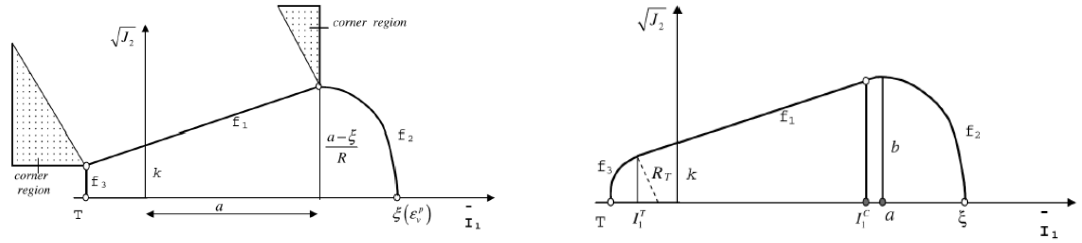

(a) (b)

Fig. 2 Cap model (a) non-smooth cap model (b) modified cap model (Dolarevic and Ibrahimbegovic 2007)

4. Numerical simulations

In this section we give the results obtained for a set of numerical examples. First, we simulate the direct shear test commonly used in geotechnical engineering to determine strength parameters of soil and weak rocks. Second, we simulate the response of the soil under both rigid and flexible footing. The mesh in all examples is generated in GMSH using Delaunay triangulation (Geuzine

mid-height of the specimen is pre-imposed with the test set-up. The formed macrocrack in numerical simulation, shown in Fig. 5, splits the specimen in two parts as in experimental direct shear tests.

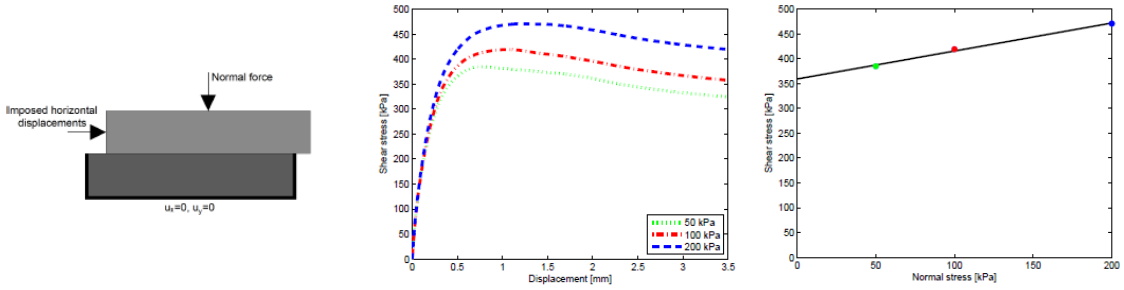

(a) (b) (c)

Fig. 4 Direct shear test: (a) loading and boundary conditions (b) computed stress - displacement curves (c) computed Mohr-Coulomb envelope

(a) (b)

Fig. 5 Elements with increasing damage (a) mode I (b) mode II (note that we mark the cohesive links that are activated by cracks)

We also preform a numerical simulation of a direct shear test on a specimen with dimensions 100×25 mm. The value of normal pressure for which we do the computation is 100 kPa. The mesh density is similar to the one used in previous computations with a total of 611 elements compared to 572 elements in the mesh shown in Fig. 3(a). In Fig. 6(a), the computed stress-displacement curves for specimens sizes 100×25 mm and 60×25 mm are shown. The specimen with dimensions 100×25 mm is slightly more resistant in the post-peak part of the response. This finding is in agreement with the probability-based explanation of the size effect (Ibrahimbegovic *et al*. 2010).

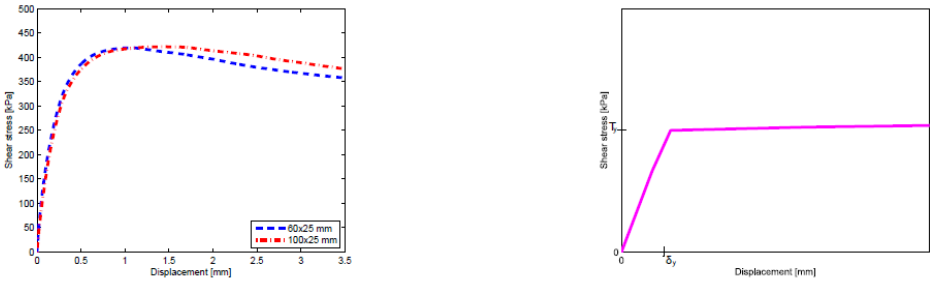

(a) (b)

Fig. 6(a) Comparison of stress-displacement curves in direct shear tests for two types of specimens (b) Typical stress-displacement curve obtained with cap model

Table 2 Mechanical properties of the Timoshenko beam finite element

Young's modulus (MPa)	Poisson's ratio	Yield limit (MPa)	Hardening modulus (MPa)	Fracture limit (MPa)	Fracture energy (MN/m)
$E=160$	$v=0.3$	$\sigma_{y,t}=0.03$	$K_t=60$	$\sigma_{u,t}=0.09$	$G_{f,t}=0.0006$
		$\sigma_{y,c}=0.30$	$K_c=60$	$\sigma_{u,c}=0.90$	$G_{f,c}=0.06$
		$\sigma_{y,s}=0.07$	$K_s=60$	$\sigma_{u,s}=0.13$	$G_{f,s}=0.02$

Computed reaction-displacement curves are shown in Fig. 9. Linear elastic parts of the responses for the coarse and the fine mesh do not differ significantly. After first cracks start to form, responses for two different types of the mesh start to differ in the end resulting with the different ultimate load values. In the post-peak behavior, a macrocrack of a similar pattern is formed in both cases, leading to the failure of soil under the footing. The macrocrack propagation occurs dominantly in mode II in the case of the coarse mesh, whereas in the case of the fine mesh macrocrack propagation occurs in both modes I and II. The shape of the formed macrocrack under the footing corresponds to the commonly observed shape of the failure wedge (Figs. 10, 11).

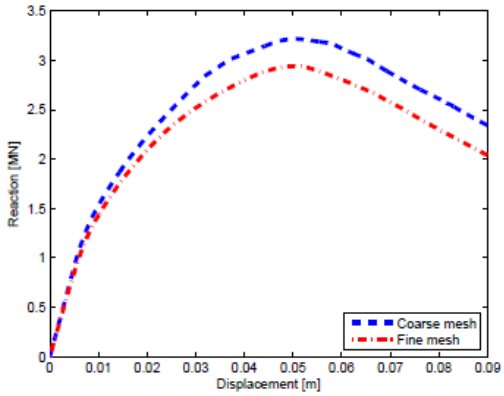

Fig. 9 Comparison of computed force-displacement curves for rigid footing

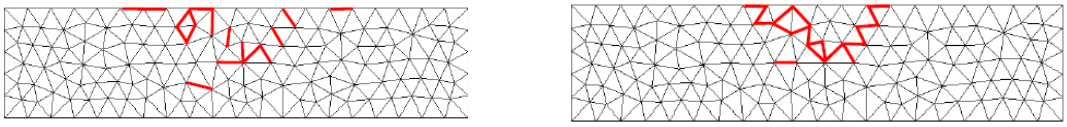

(a) (b)

Fig. 10 Coarse mesh: Elements with increasing damage (a) mode I (b) mode II

(a) (b)

Fig. 11 Fine mesh: Elements with increasing damage (a) mode I (b) mode II

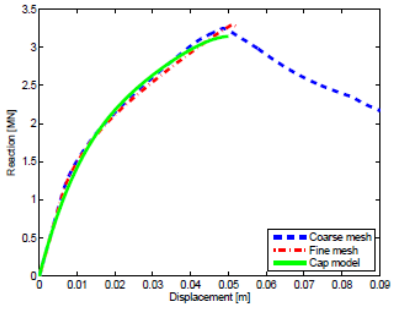

Fig. 12 Comparisson of the computed force-displacement curve with the curve provided by the modified cap model for flexible footing

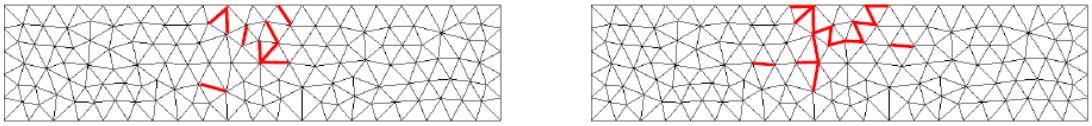

(a) (b)

Fig. 13 Coarse mesh: Elements with increasing damage (a) mode I (b) mode II

(a) (b)

Fig. 14 Fine mesh: Elements with increasing damage (a) mode I (b) mode II

In the Fig. 15, stress states under footing obtained with the modified cap model in (Dolarevic and Ibrahimbegovic 2008) are shown. We can conclude that a failure wedge of similar shape as in the case of the discrete model is also noticed. However, the plastic zone in the cap model is smeared across a large area of the domain.

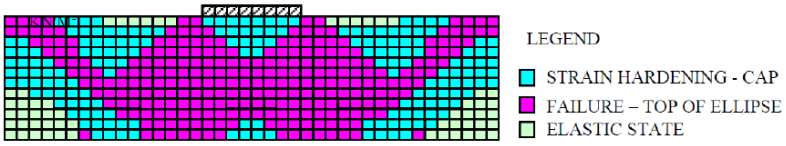

Fig. 15 Stress state under footing for modified cap model (Dolarevic and Ibrahimbegovic 2008)

To compare the results for rigid and flexible footing, we repeat computation for flexible footing with the values of mechanical properties of the Timoshenko beam finite element given in table 2. From computed curves, shown in figure 16, we can state that the value of ultimate load is higher in the case of a rigid footing. We can also conclude that the response of the discrete beam lattice model exibits some mesh dependency. A certain level of mesh-dependency is also observed in the continuum model in (Dolarevic and Ibrahimbegovic 2007).

References

Benkemoun, N., Hautefeuille, M., Colliat J.B. and Ibrahimbegovic, A. (2010), "Failure of heterogeneous materials: 3D meso-scale FE models with embedded discontinuities", *J. Numer. Meth. Eng.*, **2010**(82), 1671-1688.

Benkemoun, N., Ibrahimbegovic, A. and Colliat, J.B. (2010), "Anisotropic constitutive model of plasticity capable of accounting for details of meso-structure of two-phase composite material", *Comput. Struct.*, **2012**(90), 153-162.

Callari, C. and Armero, F. (2004), "Analysis and numerical simulation of strong discontinuities in finite strain poroplasticity", *Comput. Meth. Appl. Mech. Eng.*, **2004**(193), 2941-2986.

Callari, C., Armero, F. and Abati, A. (2010), "Strong discontinuities in partially saturated poroplastic solids", *Comput. Meth. Appl. Mech. Eng.*, **2010**(199), 1513-1535.

Chore, H.S. (2014), "Interactive analysis of a building fame resting on pile foundation", *Coupled Syst. Mech.*, **2014**(3), 367-384.

Chore, H.S. and Siddiqui, M.J. (2016), "Soil-structure interaction analysis of a building frame supported on piled raft", *Coupled Syst. Mech.*, **2016**(5), 41-58.

Conte, E., Donato, A. and Torncone, A. (2013), "Progressive failure analysis of shallow foundations on soils with strain-softening behaviour", *Comput. Geotech.*, **2013**(54), 117-124.

Conte, E., Silvestri F. and Torncone A. (2010), "Stability analysis of slopes in soils with strain-softening behaviour", *Comput. Geotech.*, **2010**(37), 710-722.

DiMaggio, F.L. and Sandler, I.S. (1971), "Material models for granular soils", *J. Eng. Mech. Div.*, **1971**(97), 935-950.

Do, X.N., Ibrahimbegovic, A. and Brancherie, D. (2015), "Combined hardening and localized failure with softening plasticity in dynamics", *Coupled Syst. Mech.*, **2015**(4), 115-136.

Doherty, J.P. and Muir Wood, D. (2015), "An extended Mohr-Coulomb (EMC) model for predicting the settlement of shallow foundations on sand, *Géotech.*, **2013**(63), 661-673.

Dolarevic, S. and Ibrahimbegovic, A. (2008), "Nonlinear behavior of soil as the source of structure damages", *Proceedings of the NATO-ARW Damage Assessment and Reconstruction after Natural Disasters and Previous Military Activities*, Sarajevo, October.

Dolarevic, S. and Ibrahimbegovic, A. (2007), "A modified three-sruface elasto-plastic cap model and its numerical implementation", *Comput. Struct.*, **2007**(85), 419-430.

Edelsbrunner, H. (2001), *Geometry and Topology for Mesh Generation*, Cambridge University Press.

Geuzaine, C. and Remache, J.F. (2009), "Gmsh: A 3-D finite element mesh generator with built-in pre- and post-processing facilities", *J. Numer. Meth. Eng.*, **2009**(79), 1309-1331.

Hofstetter, G., Simo, J.C. and Taylor, R.L. (1993), "A modified cap model: Closest point solution alghoritms", *Comput. Struct.*, **1993**(48), 203-214.

Ibrahimbegovic, A. (2009), *Nonlinear Solid Mechanics: Theoretical Formulations and Finite Element Solution Methods*, Springer.

Ibrahimbegovic, A., Colliat, J.B., Hautefeuille, M., Brancherie, D. and Melnyk S. (2010), "Probability based size effect representation for failure in civil engineering structures built of heterogeneous materials", *Comput. Meth. Stochast. Dyn.*, **2010**(22), 291-313.

Ibrahimbegovic, A. and Delaplace, A. (2003), "Microscale and mesocale discrete models for dynamic fracture of structures built of brittle material", *Comput. Struct.*, **2003**(81), 1255-1265.

Ibrahimbegovic, A., Markovic, D. and Gatuingt, F. (2003), "Constitutive model of coupled damage-plasticity and its finite element implementation", *Revue Eurpéenne des Eléments Finis*, **2003**(12), 381-405.

Imamovic, I., Ibrahimbegovic, A., Knopf-Lenoir, C. and Mesic, E. (2015), "Plasticity-damage model parameters identification for structural connections", *Coupled Syst. Mech.*, **2015**(4), 337-364.

Nikolic, M. and Ibrahimbegovic, A. (2015), "Rock mechanics model capable of representing initial heterogeneities and full set of 3D failure mechanisms", *Comput. Meth. Appl. Mech. Eng.*, **2015**(290), 209-227.

Nikolic, M., Ibrahimbegovic, A. and Miscevic, P. (2015), "Brittle and ductile failure of rocks: Embedded discontinuity approach for representing mode I and mode II failure mechanisms", *J. Numer. Meth. Eng.*, **2015**(102), 1507-1526.

Saksala, T., Brancherie, D., Harari, I. and Ibrahimbegovic, A. (2015), "Combined continuum damage-embedded discontinuity model for explicit dynamic fracture analyses of quasi-brittle materials", *J. Numer. Meth. Eng.*, **2015**(101), 230-250.

Saksala, T., Brancherie, D. and Ibrahimbegovic, A. (2016), "Numerical modeling of dynamic rock fracture with a combined 3D continuum viscodamage-embedded discontinuity model", *J. Numer. Anal. Meth. Geomech.*, **2016**(40), 1339-1357.

Saksala, T. and Ibrahimbegovic, A. (2014), "Anisotropic viscodamage-viscoplastic consistency constitutive model with a parabolic cap for rocks with brittle and ductile behavior", *J. Rock Mech. Min. Sci.*, **2014**(70), 460-473.

Schanz, T., Vermeer, P.A. and Bonnier, P.G. (1999), "The Hardening soil model: Formulation and verification", *Proceedings of the Plaxis-Symposium: Beyond 2000 in Computational Geotechnics*, Amsterdam, **1999**, 281-296.

Truty, A. and Obrzud, R. (2015), "Improved formulation of the hardening soil model in the context of modeling the undrained behavior of cohesive soils", *Stud. Geotech. Mech.*, 2**015**(37), 61-68.

Zienkiewicz, O.C. and Taylor, R.L. (2005), *The Finite Element Method, Vols. I, II, III*, Elsevier.

AI